

Mixed quantum-classical equilibrium

Priya V. Parandekar and John C. Tully

Citation: *J. Chem. Phys.* **122**, 094102 (2005); doi: 10.1063/1.1856460

View online: <http://dx.doi.org/10.1063/1.1856460>

View Table of Contents: <http://jcp.aip.org/resource/1/JCPSA6/v122/i9>

Published by the American Institute of Physics.

Additional information on J. Chem. Phys.

Journal Homepage: <http://jcp.aip.org/>

Journal Information: http://jcp.aip.org/about/about_the_journal

Top downloads: http://jcp.aip.org/features/most_downloaded

Information for Authors: <http://jcp.aip.org/authors>

ADVERTISEMENT



Submit Now

Explore AIP's new open-access journal

- Article-level metrics
now available
- Join the conversation!
Rate & comment on articles

Mixed quantum-classical equilibrium

Priya V. Parandekar and John C. Tully

Department of Chemistry, Yale University, New Haven, Connecticut 06520-8107

(Received 15 November 2004; accepted 14 December 2004; published online 24 February 2005)

We present an analysis of the equilibrium limits of the two most widely used approaches for simulating the dynamics of molecular systems that combine both quantum and classical degrees of freedom. For a two-level quantum system connected to an infinite number of classical particles, we derive a simple analytical expression for the equilibrium mean energy attained by the self-consistent-field (Ehrenfest) method and show that it deviates substantially from Boltzmann. By contrast, “fewest switches” surface hopping achieves Boltzmann quantum state populations. We verify these analytical results with simulations. © 2005 American Institute of Physics.

[DOI: 10.1063/1.1856460]

I. INTRODUCTION

Molecular dynamics (MD), the numerical simulation of the classical mechanical equations of motion of a collection of atoms interacting via a first principles or empirical force field, has become a powerful tool for investigating the equilibrium and dynamical properties of molecular systems of interest in physics, chemistry, engineering, materials science, and biology. MD has two fundamental limitations. First, it is based on the Born–Oppenheimer approximation;¹ the force field is derived from the potential energy surface corresponding to a single electronic state. Second, atoms evolve by classical mechanics instead of quantum mechanics. One approach for addressing both of these shortcomings is to introduce quantum mechanical degrees of freedom that are coupled to the classical motion. The quantum degrees of freedom may be electronic to incorporate nonadiabatic transitions between different electronic states,² and/or they may be selected atomic motions, for example, to describe tunneling and zero-point motion effects when simulating proton transfer.³ A required attribute of any such mixed quantum-classical (MQC) scheme is proper inclusion of feedback between the quantum and classical degrees of freedom.^{4,5} The motion of the classical particles imparts a time dependence into the quantum Hamiltonian that stimulates quantum transitions. Quantum state changes, in turn, alter the forces acting on the classical particles (the “quantum back reaction” on the classical system). Self-consistency between the classical and quantum particles must be treated properly. This has proved to be a difficult challenge. Two general approaches have emerged for including quantum-classical feedback in MQC simulations, the self-consistent field (Ehrenfest) method⁶ and surface hopping.⁷ Both methods incorporate quantum transitions driven by classical motion, both properly conserve total quantum plus classical energy, and both include quantum coherence effects. While they have proved useful and accurate in many contexts, both have well-studied shortcomings.^{4,8,9} One potential shortcoming that has not received much attention is the extent to which these methods satisfy detailed balance;^{4,8,10} i.e., does the MQC dynamics approach the correct equilibrium state? It is well known that

a quantum system in contact with a classical bath does not approach the correct equilibrium state. Rather, forward and backward transition probabilities are equal, resulting in equal populations of all quantum states; i.e., the quantum subsystem approaches infinite temperature.¹¹ This is a general result, usually presented as a consequence of the commutation of classical operators. This result does not apply to either the Ehrenfest or surface hopping theories, however. This can be easily demonstrated. With both methods the sum of the energies of the classical and quantum subsystems is properly conserved. If the total energy of the combined system is less than that required to excite the quantum subsystem to a particular quantum state, then that state cannot be fully populated without violation of energy conservation. Any canonical ensemble average must then include some low-energy contributions for which quantum states are unequally populated. This argument is not helpful, however, in determining the canonical ensemble average populations of quantum levels in MQC dynamics. We examine this question here for a two-level quantum system connected to a large (infinite) number of classical particles.

II. QUANTUM SUBSYSTEM

The two-level quantum subsystem is described in an adiabatic basis. The wave functions α_q and β_q are the eigenfunctions of the quantum Hamiltonian for fixed classical position \mathbf{q} ,

$$\mathcal{H}_q \alpha_q = \varepsilon_\alpha(\mathbf{q}) \alpha_q \quad (1a)$$

and

$$\mathcal{H}_q \beta_q = \varepsilon_\beta(\mathbf{q}) \beta_q. \quad (1b)$$

The subscript q indicates that the quantum Hamiltonian and its eigenfunctions depend parametrically on the classical positions \mathbf{q} . The eigenenergies $\varepsilon_\alpha(\mathbf{q})$ and $\varepsilon_\beta(\mathbf{q})$ in general are also functions of \mathbf{q} ; they are the usual adiabatic potential energy surfaces for states α and β . We express the wave function of the quantum subsystem as a linear combination of α_q and β_q ,

$$\psi(t) = c_\alpha(t)\alpha_q + c_\beta(t)\beta_q, \quad (2)$$

where $c_\alpha(t)$ and $c_\beta(t)$ are the complex-valued expansion coefficients. Substituting Eq. (2) into the time-dependent Schrödinger equation gives the usual set of coupled differential equations for the time-varying amplitudes $c_\alpha(t)$ and $c_\beta(t)$,

$$dc_\alpha/dt = -\frac{i}{\hbar}\varepsilon_\alpha c_\alpha - \dot{\mathbf{q}} \cdot \mathbf{d}_{\alpha\beta} c_\beta, \quad (3)$$

$$dc_\beta/dt = -\frac{i}{\hbar}\varepsilon_\beta c_\beta + \dot{\mathbf{q}} \cdot \mathbf{d}_{\alpha\beta} c_\alpha, \quad (4)$$

where we have assumed for simplicity of notation that the adiabatic wave functions α_q and β_q are real valued. The nonadiabatic coupling vector $\mathbf{d}_{\alpha\beta}$ is given by

$$\mathbf{d}_{\alpha\beta} = \langle \alpha_q | \nabla_q \beta_q \rangle. \quad (5)$$

Thus, the coupling between the quantum and classical subsystems is proportional to the dot product of the classical velocity vector $\dot{\mathbf{q}}$ and the nonadiabatic coupling vector $\mathbf{d}_{\alpha\beta}$. Potential energy terms coupling the quantum and classical subsystems are eliminated by our choice of the adiabatic representation, Eq. (1). From Eqs. (3) and (4), we obtain

$$d|c_\alpha|^2/dt = -\dot{\mathbf{q}} \cdot \mathbf{d}_{\alpha\beta}(c_\alpha^* c_\beta + c_\beta^* c_\alpha), \quad (6)$$

$$d|c_\beta|^2/dt = \dot{\mathbf{q}} \cdot \mathbf{d}_{\alpha\beta}(c_\alpha^* c_\beta + c_\beta^* c_\alpha). \quad (7)$$

Summing Eqs. (6) and (7) demonstrates conservation of norm.

In order to investigate the equilibrium behavior of the MQC methods, we define two new variables, X and Y , in terms of the quantum amplitudes,

$$X = |c_\beta|^2 = 1 - |c_\alpha|^2, \quad (8)$$

$$Y = c_\alpha^* c_\beta + c_\beta^* c_\alpha. \quad (9)$$

From Eqs. (3), (4), and (7) we obtain

$$\dot{X} = \dot{\mathbf{q}} \cdot \mathbf{d}_{\alpha\beta} Y, \quad (10)$$

$$\dot{Y} = \mp [(\varepsilon_\beta - \varepsilon_\alpha)/\hbar] \sqrt{4X - 4X^2 - Y^2} + 2\dot{\mathbf{q}} \cdot \mathbf{d}_{\alpha\beta}(1 - 2X). \quad (11)$$

The variables X and Y are closely related to the “effective classical variables” of the semiclassical theory of nonadiabatic dynamics developed by Meyer and Miller.¹² Equations (10) and (11) describe the evolution of the quantum subsystem, equivalent to Eqs. (3) and (4). The square root term in Eq. (11) is proportional to the imaginary part of $c_\alpha c_\beta^*$ and can be either positive or negative. The existence of two roots might complicate the use of Eq. (11) to propagate the quantum equations of motion, but it does not affect determination of the equilibrium limits as long as the contributions from both roots are included.

III. MIXED QUANTUM-CLASSICAL EQUILIBRIUM

In order to derive analytical expressions for the equilibrium properties of MQC theories, we examine the following

model system: The classical subsystem is a linear chain of N atoms, all of mass m , interacting among each other via a potential energy function $V(\mathbf{q})$, where \mathbf{q} and \mathbf{p} denote the positions and momenta of the classical particles, respectively. The quantum subsystem is a two-level system coupled to atom 1 of the classical chain. The assumption that the quantum subsystem is coupled only to the first atom of the chain is for simplicity only, it does not affect any of the conclusions but allows the term $\dot{\mathbf{q}} \cdot \mathbf{d}_{\alpha\beta}$ to be replaced by $p_1 d_{\alpha\beta}/m$. The quantum energy levels ε_α and ε_β and nonadiabatic coupling strength $d_{\alpha\beta}$ are taken to be independent of \mathbf{q} .

A. No quantum back reaction

We first examine the case where there is no quantum back reaction, i.e., the motions of the classical particles drive quantum transitions but the classical motion is unaffected by these transitions. The equations of motion for this model are

$$\dot{X} = p_1 d_{\alpha\beta} Y/m, \quad (12)$$

$$\dot{Y} = \mp [(\varepsilon_\beta - \varepsilon_\alpha)/\hbar] \sqrt{4X - 4X^2 - Y^2} + 2p_1 d_{\alpha\beta}(1 - 2X)/m, \quad (13)$$

$$\dot{q}_i = p_i/m, \quad i = 1, N, \quad (14)$$

$$\dot{p}_i = -\frac{\partial V(\mathbf{q})}{\partial q_i}, \quad i = 1, N. \quad (15)$$

Equations (12) and (13), which follow from Eqs. (10) and (11), are the classical-like equations of motion for the continuous variables X and Y describing the quantum subsystem. Equations (14) and (15) are Hamilton's equations for the N classical positions and momenta, q_i and p_i . Following McQuarrie,¹³ e.g., Eqs. (12)–(15) produce the following partial differential equation for the time evolution of the probability distribution $f(\mathbf{q}, \mathbf{p}, X, Y)$ of the variables \mathbf{q} , \mathbf{p} , X , and Y :

$$\begin{aligned} \frac{\partial f}{\partial t} = & - \sum_{i=1}^N \left[\frac{p_i}{m} \frac{\partial f}{\partial q_i} - \frac{\partial V}{\partial q_i} \frac{\partial f}{\partial p_i} \right] - (p_1 d_{\alpha\beta} Y/m) \frac{\partial f}{\partial X} \\ & - (2p_1 d_{\alpha\beta}/m)(1 - 2X) \frac{\partial f}{\partial Y} + \left[\frac{\varepsilon_\beta - \varepsilon_\alpha}{\hbar} \right] \\ & \times \left[(4X - 4X^2 - Y^2)^{1/2} \frac{\partial f}{\partial Y} - Y(4X - 4X^2 - Y^2)^{-1/2} f \right]. \end{aligned} \quad (16)$$

The term in the summation in Eq. (16) is the standard Liouville equation for the classical particles, confirming that for this case the classical trajectory is not affected by the quantum variables X and Y . To obtain the equilibrium distribution we set $\partial f/\partial t = 0$ in Eq. (16),

$$\sum_{i=1}^N \left[\frac{p_i}{m} \frac{\partial f}{\partial q_i} - \frac{\partial V}{\partial q_i} \frac{\partial f}{\partial p_i} \right] + (p_1 d_{\alpha\beta} Y/m) \frac{\partial f}{\partial X} + (2p_1 d_{\alpha\beta}/m) \times (1-2X) \frac{\partial f}{\partial Y} - \left[\frac{\varepsilon_\beta - \varepsilon_\alpha}{\hbar} \right] \left[(4X - 4X^2 - Y^2)^{1/2} \times \frac{\partial f}{\partial Y} - Y(4X - 4X^2 - Y^2)^{-1/2} f \right] = 0. \quad (17)$$

Enforcing a Maxwellian distribution for the classical momenta p_i , the canonical ensemble equilibrium distribution function $f(\mathbf{q}, \mathbf{p}, X, Y)$ is given by

$$f(\mathbf{q}, \mathbf{p}, X, Y) = A \exp[-V(\mathbf{q})/k_B T] \times \prod_{i=1}^N \exp[-p_i^2/2mk_B T] g(X, Y), \quad (18)$$

where A is a normalization constant, T is the temperature of the classical chain, k_B is the Boltzmann constant, and

$$g(X, Y) = (1/\pi)(4X - 4X^2 - Y^2)^{-1/2}. \quad (19)$$

This solution can be verified by substitution of Eqs. (18) and (19) into Eq. (17). Equation (19) is the canonical ensemble distribution function for the effective classical variables X and Y . This expression can be integrated over Y to obtain the distribution of the variable X , i.e., the probability distribution of $|c_\beta|^2$,

$$g_X(X) = \int_{-(4X-4X^2)^{1/2}}^{(4X-4X^2)^{1/2}} \frac{1}{\pi} (4X - 4X^2 - Y^2)^{-1/2} dY = 1. \quad (20)$$

The limits of integration result from the inequality

$$Y^2 = (c_\alpha^* c_\beta + c_\alpha c_\beta^*)^2 \leq 4|c_\alpha|^2 |c_\beta|^2 = 4X - 4X^2. \quad (21)$$

Equation (20) shows that not only are the average populations of states α and β equal (infinite temperature), $\langle X \rangle = \langle |c_\beta|^2 \rangle = \langle |c_\alpha|^2 \rangle = 1/2$, but the equilibrium distribution of $|c_\beta|^2$ is uniform over the interval $0 < |c_\beta|^2 < 1$. This is an alternative proof of the statement that a quantum system coupled to a classical bath approaches infinite temperature. This is true, however, only if the classical trajectory is not affected by changes in the quantum amplitudes; i.e., only if there is no quantum back reaction. Both the Ehrenfest and surface hopping theories include quantum back reaction, but in different ways.

B. Ehrenfest

We next examine the Ehrenfest method for which the potential energy function governing the classical subsystem is an average of the adiabatic potential energy surfaces for each quantum state, weighted by the square of the absolute value of the amplitude of the state,

$$\begin{aligned} \dot{\mathbf{p}}(t) &= -\nabla_{\mathbf{q}} V(\mathbf{q}) - \nabla_{\mathbf{q}} \langle \psi(t) | \mathcal{H}_q | \psi(t) \rangle \\ &= -\nabla_{\mathbf{q}} V(\mathbf{q}) - (c_\alpha^* c_\beta + c_\beta^* c_\alpha)(\varepsilon_\beta - \varepsilon_\alpha) \mathbf{d}_{\alpha\beta} \\ &\quad - |c_\alpha|^2 \nabla_{\mathbf{q}} \varepsilon_\alpha - |c_\beta|^2 \nabla_{\mathbf{q}} \varepsilon_\beta. \end{aligned} \quad (22)$$

The simultaneous propagation of the classical equations of motion, Eq. (22), along with Eqs. (3) and (4) for the quantum

amplitudes, defines the Ehrenfest method for the two-level case. Note that quantum transitions—changes in the quantum amplitudes—produce an effective force on the classical particles in the direction of the nonadiabatic coupling vector \mathbf{d} . For our model two-level system in which the quantum system is coupled only to p_1 and the energy splitting $\varepsilon_\beta - \varepsilon_\alpha$ is constant, the equations of motion are

$$\dot{X} = p_1 \cdot d_{\alpha\beta} Y/m, \quad (23)$$

$$\dot{Y} = \mp [(\varepsilon_\beta - \varepsilon_\alpha)/\hbar] \sqrt{4X - 4X^2 - Y^2} + 2p_1 d_{\alpha\beta} (1 - 2X)/m, \quad (24)$$

$$\dot{q}_i = p_i/m, \quad i = 1, N, \quad (25)$$

$$\dot{p}_1 = -\frac{\partial V(\mathbf{q})}{\partial q_1} - (\varepsilon_\beta - \varepsilon_\alpha) d_{\alpha\beta} Y, \quad (26)$$

$$\dot{p}_i = -\frac{\partial V(\mathbf{q})}{\partial q_i}, \quad i = 2, N. \quad (27)$$

The only change from Eqs. (12)–(15) is Eq. (26) for classical particle number 1. Equation (17) is then modified as follows:

$$\begin{aligned} \sum_{i=1}^N \left[\frac{p_i}{m} \frac{\partial f}{\partial q_i} - \frac{\partial V}{\partial q_i} \frac{\partial f}{\partial p_i} \right] + (p_1 d_{\alpha\beta} Y/m) \frac{\partial f}{\partial X} + (2p_1 d_{\alpha\beta}/m) \times (1-2X) \frac{\partial f}{\partial Y} - \left[\frac{\varepsilon_\beta - \varepsilon_\alpha}{\hbar} \right] \left[(4X - 4X^2 - Y^2)^{1/2} \frac{\partial f}{\partial Y} - Y(4X - 4X^2 - Y^2)^{-1/2} f \right] - (\varepsilon_\beta - \varepsilon_\alpha) d_{\alpha\beta} Y \frac{\partial f}{\partial p_1} = 0. \end{aligned} \quad (28)$$

The resulting equilibrium distribution $f(\mathbf{q}, \mathbf{p}, X, Y)$ is

$$f(\mathbf{q}, \mathbf{p}, X, Y) = A \exp[-V(\mathbf{q})/k_B T] \times \prod_{i=1}^N \exp[-p_i^2/2mk_B T] g(X, Y), \quad (29)$$

where A is a normalization constant and

$$g(X, Y) = (1/\pi)(4X - 4X^2 - Y^2)^{-1/2} \exp[-(\varepsilon_\beta - \varepsilon_\alpha)X/k_B T]. \quad (30)$$

This solution can be verified by substitution of Eqs. (29) and (30) into Eq. (28). Equation (30) can be integrated over Y to obtain the distribution of the variable X , the unnormalized probability distribution of $|c_\beta|^2$,

$$\begin{aligned} g_X(X) &= \int_{-(4X-4X^2)^{1/2}}^{(4X-4X^2)^{1/2}} \frac{1}{\pi} (4X - 4X^2 - Y^2)^{-1/2} \\ &\quad \times \exp[-(\varepsilon_\beta - \varepsilon_\alpha)X/k_B T] dY \\ &= \exp[-(\varepsilon_\beta - \varepsilon_\alpha)X/k_B T], \quad 0 < X < 1. \end{aligned} \quad (31)$$

Therefore, in the case where the energy splitting $\varepsilon_\beta - \varepsilon_\alpha$ is independent of \mathbf{q} , the population of the excited state, $X = |c_\beta|^2$, is given by a truncated classical Boltzmann distribution. The distribution is truncated because $|c_\beta|^2$ can never be greater than unity. Substituting $|c_\beta|^2$ for X , the mean popula-

tion of the excited state at equilibrium is given by

$$\begin{aligned} \langle |c_\beta|^2 \rangle &= \frac{\int_0^1 |c_\beta|^2 g_x(|c_\beta|^2) d|c_\beta|^2}{\int_0^1 g_x(|c_\beta|^2) d|c_\beta|^2} \\ &= \frac{k_B T}{\epsilon_\beta - \epsilon_\alpha} - \frac{\exp[-(\epsilon_\beta - \epsilon_\alpha)/k_B T]}{1 - \exp[-(\epsilon_\beta - \epsilon_\alpha)/k_B T]}, \end{aligned} \quad (32)$$

and the mean energy E_Q of the quantum subsystem is

$$\begin{aligned} \langle E_Q \rangle &= \langle |c_\alpha|^2 \rangle \epsilon_\alpha + \langle |c_\beta|^2 \rangle \epsilon_\beta \\ &= \epsilon_\alpha + k_B T - \frac{(\epsilon_\beta - \epsilon_\alpha) \exp[-(\epsilon_\beta - \epsilon_\alpha)/k_B T]}{1 - \exp[-(\epsilon_\beta - \epsilon_\alpha)/k_B T]}. \end{aligned} \quad (33)$$

The high temperature limits of Eqs. (32) and (33), obtained by expanding the exponentials in a series, are $\langle |c_\beta|^2 \rangle = 1/2$ and $\langle E_Q \rangle = (\epsilon_\alpha + \epsilon_\beta)/2$.

To verify these expressions we have carried out numerical simulations of the two-level, linear chain model with the following anharmonic, nearest-neighbor potential energy function:

$$V(\mathbf{q}) = \sum_{k=1}^N V_M(q_k - q_{k+1}), \quad (34)$$

where

$$V_M(q) = V_0(a^2 q^2 - a^3 q^3 + 0.58a^4 q^4) \quad (35)$$

and q_{N+1} is a fixed position. The coefficients in Eq. (35) were chosen to approximate the attractive well region of a Morse potential. The number of classical atoms in the chain was typically chosen to be 20. In addition, a Langevin friction constant γ and white random force $F(t)$ were imposed on atom number N of the chain, the one most distant from the quantum subsystem, in order to ensure that the classical subsystem achieved the correct canonical ensemble equilibrium. $F(t)$ is a Gaussian random variable of width given by¹⁴

$$\sigma = (2\gamma m k_B T \delta^{-1})^{1/2}, \quad (36)$$

where δ is the time step of the integration. The classical equations of motion were integrated using a modified Beeman algorithm.^{14,15} The quantum equations of motion, Eqs. (3) and (4), were integrated using the fourth-order Runge-Kutta algorithm.¹⁶ The Ehrenfest results were obtained from an ensemble of 20 trajectories, each 50 ps in length, with a time step of 0.001 fs. The initial 20 ps was neglected in the averages to remove any dependence on initial conditions. The values of all parameters are listed in Table I. Simulations were also carried out for an isolated system, i.e., with no random force and friction. When the number of classical atoms, N , was chosen large enough to provide an adequate heat bath, the isolated system results were the same as those of Fig. 1 for the open system. The open system is more convenient, however, when the quantum energy splitting is large, $(\epsilon_\beta - \epsilon_\alpha) \gg k_B T$, where a very large number of classical atoms would be required to obtain accurate canonical ensemble averages from an isolated system calculation.

TABLE I. Values of the parameters used in the simulations.

Parameter	Value
N	20
m	12 amu
V_0	175 kJ/mol
a	4 Å ⁻¹
γ	10 ¹⁴ s ⁻¹
$\Delta = \epsilon_\beta - \epsilon_\alpha$	34.6 kJ/mol
$d_{\alpha\beta}$	-6.5 Å ⁻¹

As shown in Fig. 1, the mean population of the excited level, $\langle |c_\beta|^2 \rangle$, as computed by the Ehrenfest method, is indeed given by Eq. (32), within statistical uncertainty. This result is contrasted to that of a quantum Boltzmann distribution:

$$\langle |c_\beta|^2 \rangle = \frac{\exp[-(\epsilon_\beta - \epsilon_\alpha)/k_B T]}{1 + \exp[-(\epsilon_\beta - \epsilon_\alpha)/k_B T]}. \quad (37)$$

When $(\epsilon_\beta - \epsilon_\alpha) \gg k_B T$, the Ehrenfest equilibrium quantum state populations deviate dramatically from Boltzmann. Thus the equilibrium state achieved by the Ehrenfest method, while not infinite in temperature, nonetheless is very unrealistic.

C. Surface hopping

In addition to its incorrect long-time limit as just discussed, the Ehrenfest method suffers from the same deficiency as all mean field approximations, it does not include correlation; i.e., classical motion follows a single average path. The surface hopping method was developed to address this deficiency by allowing a trajectory to split into branches, each quantum state giving rise to a different branch governed

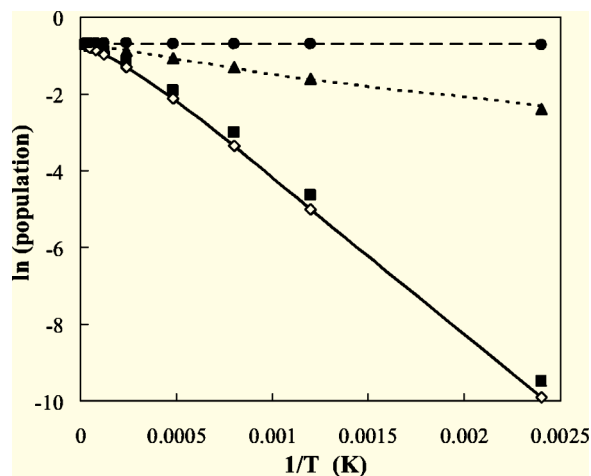


FIG. 1. Equilibrium populations of the excited state of the two-level, linear chain model as a function of temperature. Solid line is the quantum Boltzmann result, Eq. (37). Filled squares are the populations (mean fraction of trajectories in the excited state) generated by the surface hopping simulations. Open diamonds are the mean populations generated by surface hopping with higher nonadiabatic coupling ($d_{\alpha\beta} = -104$ Å⁻¹). Triangles are the mean populations generated by the Ehrenfest simulations. The short dashed line is the analytical expression derived for the Ehrenfest method, Eq. (32). The circles show the absolute value squared of the quantum amplitude, $|c_\beta|^2$, obtained by surface hopping. The long dashed line corresponds to the population at infinite temperature, equal to 0.5.

by state-specific forces and weighted by the quantum state probability.^{7,17} The surface hopping approach has been shown to be more accurate than the Ehrenfest method in many MQC applications, albeit not all.^{8,9,18} With the surface hopping method, the quantum state amplitudes evolve via Eqs. (3) and (4), just as with Ehrenfest. However, the quantum back reaction on the classical particles is treated differently. Instead of moving on a weighted average of potential energy surfaces, the classical forces are derived from the potential energy surface of a single quantum state. The quantum state can switch at any point along the trajectory according to a stochastic hopping algorithm. When a hop occurs to a quantum state of a different energy, the component of the classical velocity in the direction of the nonadiabatic coupling vector $\mathbf{d}_{\alpha\beta}$ is modified accordingly to conserve total energy. Multiple hops upward and downward can occur along a single trajectory, with the hopping algorithm designed so that, except for “frustrated hops,” the fractional time spent in each quantum state k is given by the average value of $|c_k|^2$ obtained from Eqs. (6) and (7). A frustrated hop occurs when the hopping algorithm calls for a switch from a quantum state of lower energy to one of higher energy, but there is insufficient kinetic energy in the nonadiabatic coupling coordinate to conserve total energy if the hop is completed.^{8,19} Here we follow the usual procedure: abort the hop and remain in the initial quantum state, with the result that the state populations may deviate from the absolute value squares of the quantum amplitudes.

The equation of motion for the classical particles is simply

$$\dot{\mathbf{p}}(t) = -\nabla_q V(\mathbf{q}) - \nabla_q \varepsilon_k(\mathbf{q}), \quad (38)$$

where k labels the current quantum state to which the system is assigned, and k is subject to change instantaneously according to the hopping algorithm. A number of alternative hopping algorithms have been proposed. We consider here only the most widely used of these, the “fewest switches” algorithm,¹⁷ which for the two-state case is

$$P_{\beta\alpha} = -d \ln |c_\beta|^2 / dt = -\dot{\mathbf{q}} \cdot \mathbf{d}_{\alpha\beta} (c_\alpha^* c_\beta + c_\beta^* c_\alpha) / |c_\beta|^2 \quad (39)$$

using Eq. (7), where $P_{\beta\alpha}$ is the probability per unit time of a hop from quantum state β to α . If $P_{\beta\alpha}$ is negative then $P_{\alpha\beta}$ is positive and a hop, if it occurs, will be from state α to β . Note that the hopping probability is proportional to the component of the classical velocity vector $\dot{\mathbf{q}}$ in the direction of the nonadiabatic coupling vector $\mathbf{d}_{\alpha\beta}$.

In surface hopping there is no direct feedback between the quantum amplitudes and the forces governing the trajectory; the amplitudes c_α and c_β do not appear in Eq. (38). Therefore, Eqs. (12)–(21) apply; i.e., the equilibrium mean values of the absolute value squared of the amplitudes, $|c_k|^2$, are equal for all quantum states. This result is not affected by the occasional discontinuous changes of momentum accompanying surface hops. This is confirmed by the simulations, as shown in Fig. 1. However, surface hopping requires propagating a swarm of many trajectories and the quantum state populations at any time are given by the fraction of trajectories assigned to each quantum state at that time, not by the squares of the amplitudes as with the Ehrenfest

method. The mean fraction of trajectories in each quantum state can be determined from detailed balancing. A stochastic surface hop from state β to α is accompanied by an energy-conserving change in the component of momentum in the direction of the nonadiabatic coupling vector. To be specific, we again consider the two-level, linear chain model with constant $\varepsilon_\beta - \varepsilon_\alpha$ and $\varepsilon_\alpha < \varepsilon_\beta$. The probability of transition from β to α is then

$$P_{\beta\alpha} = -d \ln |c_\beta|^2 / dt = -(p_1/m) d_{\alpha\beta} (c_\alpha^* c_\beta + c_\beta^* c_\alpha) / |c_\beta|^2 \\ = -(d_{\alpha\beta}/m) p_1 Y/X, \quad (40)$$

where X and Y are defined in Eqs. (8) and (9). The momentum \tilde{p}_1 of particle 1 after the hop from state β to α is given in terms of the momentum p_1 before the hop by

$$\tilde{p}_1 = \sqrt{p_1^2 + 2m(\varepsilon_\beta - \varepsilon_\alpha)}. \quad (41)$$

In our simulations the sign of \tilde{p}_1 was taken to be the same as that of p_1 . Reversing the sign would have no effect on the equilibrium state. The rate of transition $\mathcal{R}_{\beta\alpha} dp_1$ from state β with initial momentum between p_1 and $p_1 + dp_1$ is proportional to the product of the Maxwellian probability of momentum p_1 multiplied by $P_{\beta\alpha}$ of Eq. (40), where it is assumed that the sign of p_1 is such that $\mathcal{R}_{\beta\alpha} > 0$,

$$\mathcal{R}_{\beta\alpha}(p_1) dp_1 \propto (d_{\alpha\beta}/m) p_1 (Y/X) \exp(-p_1^2/2mk_B T) dp_1. \quad (42)$$

Changing variables from momentum to kinetic energy, $p_1 dp_1 = m dE_\beta$, gives

$$\mathcal{R}_{\beta\alpha}(E_\beta) dE_\beta \propto d_{\alpha\beta} (Y/X) \exp(-E_\beta/k_B T) dE_\beta. \quad (43)$$

Similarly, the rate of transition $\mathcal{R}_{\alpha\beta} dE_\alpha$ from state α to β is

$$\mathcal{R}_{\alpha\beta}(E_\alpha) dE_\alpha \propto d_{\alpha\beta} [Y/(1-X)] \exp(-E_\alpha/k_B T) dE_\alpha, \quad (44)$$

with momentum of opposite sign to that in Eq. (42). Conservation of energy before and after a surface hop requires that $E_\alpha - E_\beta = \varepsilon_\beta - \varepsilon_\alpha$. This is the same relation that is responsible for aborting energy-forbidden transitions, i.e., frustrated hops. Thus E_α must be greater than or equal to $\varepsilon_\beta - \varepsilon_\alpha$ for a hop to occur. Frustrated hops are therefore essential for achieving the correct equilibrium limits in surface hopping.

The equilibrium populations \mathcal{N}_α and \mathcal{N}_β of quantum states α and β are given by detailed balance, i.e., the ratio of the average forward and backward rates. Substituting $1-X$ into Eq. (19), we find that the distribution of the variable $(1-X) = |c_\alpha|^2$ is identical to that of $X = |c_\beta|^2$,

$$g[(1-X), Y] = (1/\pi) [4(1-X) - 4(1-X)^2 - Y^2]^{-1/2} \\ = g(X, Y). \quad (45)$$

Thus the mean values of Y/X and $Y/(1-X)$ are identical, and the ratio of the mean rates is simply

$$\mathcal{N}_\beta/\mathcal{N}_\alpha = \langle \mathcal{R}_{\alpha\beta}(E_\alpha) \rangle / \langle \mathcal{R}_{\beta\alpha}(E_\alpha - \varepsilon_\beta + \varepsilon_\alpha) \rangle \\ = \exp[-(\varepsilon_\beta - \varepsilon_\alpha)/k_B T]. \quad (46)$$

Surface hopping simulations were carried out using the same parameters as for the Ehrenfest simulations, as listed in Table I. The surface hopping results shown in Fig. 1 were obtained from an ensemble of 200 trajectories, each of 50 ps,

in length, with an integration time step of 0.01 fs. As before, the initial 20 ps of each trajectory was neglected in the averages to ensure complete equilibration. We verified this for both Ehrenfest and surface hopping simulations by demonstrating that the results do not depend upon the assignment of initial classical momenta and positions or initial quantum amplitudes. As shown in Fig. 1, the surface hopping simulations fall very close to the quantum Boltzmann curve. Moreover, when the nonadiabatic coupling $d_{\alpha\beta}$ is increased by a factor of 16, the surface hopping simulations reproduce the Boltzmann probabilities within statistical error. The reason for the small deviation with the lower value of $d_{\alpha\beta}$ is not clear. Weak nonadiabatic coupling produces relatively few surface hops, so statistics may not be reliable in this case. However, the simulation results do not exhibit much scatter, so it is possible that this deviation arises from numerical integration error, or perhaps with weak coupling the system has not fully achieved equilibrium during our 20 ps initialization period. In any case, the simulation results provide strong support for the validity of Eq. (46), demonstrating that the long-time equilibrium limit of surface hopping produces the correct Boltzmann populations of the quantum subsystem.

IV. CONCLUSIONS

Surface hopping, in the adiabatic basis with the fewest switches algorithm, produces a Boltzmann population of quantum states at long times for an ergodic system with an infinite number of classical degrees of freedom. We show elsewhere that this result holds for any number of quantum levels. No additional detailed balance relationships or external temperatures need to be imposed; quantum equilibrium evolves naturally simply from the classical motion. This is a remarkable result. It depends, first, on the fact that the probability distribution of the variables X and Y is separable from that of the classical momentum, Eqs. (18) and (19); i.e., momentum and quantum amplitudes are uncorrelated. Second, the mean value of the ratio Y/X appearing in the fewest switches downward hopping probability is equal to that of $Y/(1-X)$ that appears in the upward probability, as shown by Eq. (45). Third, the hopping rate is proportional to the classical momentum. Note that the latter is true only when surface hopping is applied in the adiabatic representation. We have argued on other grounds that to apply surface hopping using a diabatic representation is not justified.²⁰ This result supports that conclusion. Finally, permitting only those hops that are energy allowed is key to achieving a Boltzmann distribution; if all hops called for by Eq. (39) were completed, the populations of each quantum state would be equal to the absolute value squared of the corresponding amplitude, i.e., the quantum subsystem would approach infinite temperature. Thus frustrated hops, which have been cited as a weakness of surface hopping,^{8,19} are actually required to achieve correct equilibrium behavior.

We have examined here the special case for which the quantum energy levels are independent of the classical coordinates. This is not true in general. In a strongly coupled system, whether fully classical or fully quantum, the energy of any subsystem is not uniquely defined. In a MQC system, the energy of the quantum and classical subsystems are similarly ill defined. At best one can state that the equilibrium quantum state populations achieved by surface hopping are realistic and they are correct in the nearly separable limit. Neither of these statements is true for the Ehrenfest method. Molecular dynamics simulations have been a valuable complement to Monte Carlo simulations for computing the equilibrium properties of large assemblies of atoms, particularly when highly correlated motions render the latter method inefficient. Surface hopping can play the same role for MQC systems.

ACKNOWLEDGMENT

This work was supported by the National Science Foundation, Grant No. CHE0314208.

- ¹M. Born and R. Oppenheimer, *Ann. Phys.* **84**, 457 (1927).
- ²E. E. Nikitin, *Theory of Elementary Atomic and Molecular Processes in Gases* (Clarendon, Oxford, 1974); A. W. Jasper, C. Zhu, S. Nangia, and D. G. Truhlar, *Faraday Discuss.* **127**, 1 (2004).
- ³S. Hammes-Schiffer and J. C. Tully, *J. Chem. Phys.* **101**, 4657 (1994); A. Staib, D. Borgis, and J. T. Hynes, *ibid.* **102**, 2487 (1995); S. Consta and R. Kapral, *ibid.* **104**, 4581 (1996); S. R. Billeter, S. P. Webb, T. Iordanov, P. K. Agarwal, and S. Hammes-Schiffer, *ibid.* **114**, 6925 (2001).
- ⁴J. C. Tully, in *Modern Methods for Multidimensional Dynamics Computations in Chemistry*, edited by D. L. Thompson (World Scientific, Singapore, 1998), p. 34.
- ⁵P. Pechukas, *Phys. Rev.* **181**, 174 (1969); M. F. Herman, *Annu. Rev. Phys. Chem.* **45**, 83 (1994); O. V. Prezhdo, and C. Brooksby, *Phys. Rev. Lett.* **86**, 3215 (2001); J. C. Burant and J. C. Tully, *J. Chem. Phys.* **112**, 6097 (2001); D. M. Kernan, G. Ciccotti, and R. Kapral, *ibid.* **116**, 2346 (2002).
- ⁶A. D. McLachlan, *Mol. Phys.* **8**, 39 (1964); D. A. Micha, *J. Chem. Phys.* **78**, 7138 (1983); Z. Kirson, R. B. Gerber, A. Nitzan, and M. A. Ratner, *Surf. Sci.* **137**, 527 (1984); S. I. Sawada, A. Nitzan, and H. Metiu, *Phys. Rev. B* **32**, 851 (1985).
- ⁷J. C. Tully and R. K. Preston, *J. Chem. Phys.* **55**, 562 (1971); J. C. Tully, in *Modern Theoretical Chemistry: The Dynamics of Molecular Collisions*, edited by W. H. Miller (Plenum, New York, 1976), p. 217.
- ⁸U. Müller and G. Stock, *J. Chem. Phys.* **107**, 6230 (1997).
- ⁹D. Kohen, F. H. Stillinger, and J. C. Tully, *J. Chem. Phys.* **109**, 4713 (1998); J. Fang and S. Hammes-Schiffer, *ibid.* **110**, 11166 (1999).
- ¹⁰J. Mavri and H. J. C. Berendsen, *Phys. Rev. E* **50**, 198 (1994).
- ¹¹K. Blum, in *Density Matrix Theory and Applications* (Plenum, New York, 1996), p. 275.
- ¹²H. D. Meyer and W. H. Miller, *J. Chem. Phys.* **70**, 3214 (1979).
- ¹³D. A. McQuarrie, in *Statistical Thermodynamics* (University Science Books, Mill Valley, CA, 1973), p. 117.
- ¹⁴J. C. Tully, G. H. Gilmer, and M. Shugard, *J. Chem. Phys.* **71**, 1630 (1979).
- ¹⁵D. Beeman, *J. Comput. Phys.* **20**, 130 (1976).
- ¹⁶W. H. Press, S. A. Teukolsky, W. T. Vetterling, and B. P. Flannery, *Numerical Recipes in C*, 2nd ed. (Cambridge University Press, Cambridge, 1992).
- ¹⁷J. C. Tully, *J. Chem. Phys.* **93**, 1061 (1990).
- ¹⁸D. S. Sholl and J. C. Tully, *J. Chem. Phys.* **109**, 7702 (1998).
- ¹⁹J. Fang and S. Hammes-Schiffer, *J. Phys. Chem. A* **103**, 9399 (1999); A. W. Jasper, S. N. Stechmann, and D. G. Truhlar, *J. Chem. Phys.* **116**, 5424 (2002); A. W. Jasper and D. G. Truhlar, *Chem. Phys. Lett.* **369**, 60 (2003).
- ²⁰J. C. Tully, *Faraday Discuss.* **110**, 407 (1998).